nature medicine

Dopamine mediates vagal modulation of the immune system by electroacupuncture

Rafael Torres-Rosas[1,2], Ghassan Yehia[1], Geber Peña[1], Priya Mishra[1], Maria del Rocio Thompson-Bonilla[1,3], Mario Adán Moreno-Eutimio[4], Lourdes Andrea Arriaga-Pizano[2], Armando Isibasi[2] & Luis Ulloa[1,5]

Previous anti-inflammatory strategies against sepsis, a leading cause of death in hospitals, had limited efficacy in clinical trials, in part because they targeted single cytokines and the experimental models failed to mimic clinical settings[1–3]. Neuronal networks represent physiological mechanisms, selected by evolution to control inflammation, that can be exploited for the treatment of inflammatory and infectious disorders[3]. Here, we report that sciatic nerve activation with electroacupuncture controls systemic inflammation and rescues mice from polymicrobial peritonitis. Electroacupuncture at the sciatic nerve controls systemic inflammation by inducing vagal activation of aromatic L-amino acid decarboxylase, leading to the production of dopamine in the adrenal medulla. Experimental models with adrenolectomized mice mimic clinical adrenal insufficiency[4], increase the susceptibility to sepsis and prevent the anti-inflammatory effects of electroacupuncture. Dopamine inhibits cytokine production via dopamine type 1 (D1) receptors. D1 receptor agonists suppress systemic inflammation and rescue mice with adrenal insufficiency from polymicrobial peritonitis. Our results suggest a new anti-inflammatory mechanism mediated by the sciatic and vagus nerves that modulates the production of catecholamines in the adrenal glands. From a pharmacological perspective, the effects of selective dopamine agonists mimic the anti-inflammatory effects of electroacupuncture and can provide therapeutic advantages to control inflammation in infectious and inflammatory disorders.

Sepsis is the leading cause of mortality in noncoronary intensive care units, killing over 250,000 patients annually and accounting for 9.3% of overall deaths in the United States[1–3]. Infection, hemorrhage, resuscitation, shock, trauma and cancer contribute to severe sepsis, which is characterized by overwhelming inflammatory responses that cause multiple organ failure[2,5–8]. New antibiotics are efficient in controlling the infection, but they do not control inflammation. Currently, there is no treatment approved by the US Food and Drug Administration for severe sepsis, and most of the therapies are largely supportive. Despite the promising results obtained from inhibiting single inflammatory cytokines such as tumor necrosis factor (TNF) or high-mobility group box-1 (HMGB1) in experimental models of sepsis[2,7,8], these strategies have failed in clinical trials[9]. One explanation is that sepsis is not induced by a single cytokine and, thus, a successful treatment for sepsis may require inhibiting multiple cytokines. Recent studies indicate that the vagus nerve controls inflammation[10] and prevents lethal experimental sepsis[11,12]. Multiple investigators have already reported that the vagus nerve controls systemic inflammation in experimental ischemia and reperfusion[13–15], hemorrhage and resuscitation[15], pancreatitis[16], colitis[17], endotoxemia[10,11], septic shock and severe sepsis[18,19]. However, the clinical applications of direct vagal nerve stimulation are limited by the anesthetics and surgery required for the direct nerve stimulation. We hypothesized that electroacupuncture can be an alternative strategy for vagal stimulation. Although the use of electroacupuncture is endorsed by the US National Institutes of Health and the World Health Organization and there is growing evidence supporting its effects in postoperative and stroke rehabilitation[20–23], its mechanisms to control inflammation remain unknown[24,25].

Electroacupuncture at the ST36 Zusanli acupuncture point reduced the lipopolysaccharide (LPS)-induced serum levels of all the cytokines analyzed, including TNF, monocyte chemotactic protein-1 (MCP-1), interleukin-6 (IL-6) and interferon-γ (INF-γ) (**Fig. 1a–d**). These results indicate that electroacupuncture inhibited and did not merely delay cytokine production. The anti-inflammatory effects of electroacupuncture are voltage dependent, and electroacupuncture with a wooden toothpick or stimulation of a non-acupuncture point did not inhibit cytokine levels (**Supplementary Fig. 1a–c**). We analyzed local sensory signals using capsaicin and selective neurectomies. Capsaicin, an agonist for transient receptor potential vanilloid member-1, which interferes with nociceptive and voltage-dependent neuronal pathways, abolished the anti-inflammatory effect of electroacupuncture (**Supplementary Fig. 1d**). Surgical sectioning of the sciatic nerve, but not the common peroneal or tibial nerve, abolished the anti-inflammatory effects of electroacupuncture (**Fig. 1e**). These results

[1]Laboratory of Anti-inflammatory Signaling, Department of Surgery, Rutgers University New Jersey Medical School, Newark, New Jersey, USA. [2]Medical Research Unit on Immunochemistry, National Medical Center Siglo XXI, Mexico City, Mexico. [3]The Institute for Social Security and Services for the State's Employees Research Institute, Mexico City, Mexico. [4]Laboratory of Immunobiology, Hospital Juárez de México, Mexico City, Mexico. [5]Center of Immunology and Inflammation, Rutgers University New Jersey Medical School, Newark, New Jersey, USA. Correspondence should be addressed to L.U. (mail@luisulloa.com).

Received 7 August 2013; accepted 17 January 2014; published online 23 February 2014; doi:10.1038/nm.3479

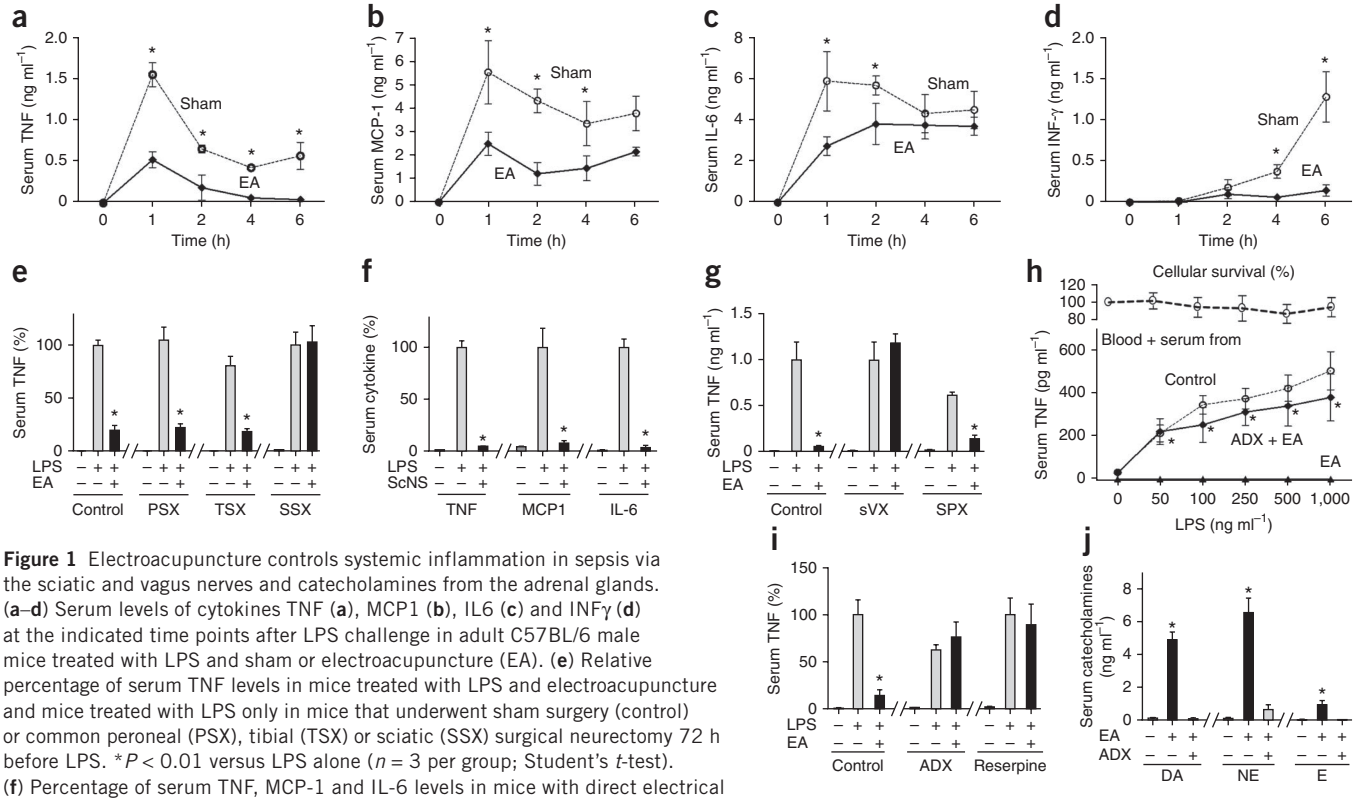

Figure 1 Electroacupuncture controls systemic inflammation in sepsis via the sciatic and vagus nerves and catecholamines from the adrenal glands. (**a**–**d**) Serum levels of cytokines TNF (**a**), MCP1 (**b**), IL6 (**c**) and INFγ (**d**) at the indicated time points after LPS challenge in adult C57BL/6 male mice treated with LPS and sham or electroacupuncture (EA). (**e**) Relative percentage of serum TNF levels in mice treated with LPS and electroacupuncture and mice treated with LPS only in mice that underwent sham surgery (control) or common peroneal (PSX), tibial (TSX) or sciatic (SSX) surgical neurectomy 72 h before LPS. $*P < 0.01$ versus LPS alone ($n = 3$ per group; Student's *t*-test). (**f**) Percentage of serum TNF, MCP-1 and IL-6 levels in mice with direct electrical sciatic nerve stimulation (ScNS) and mice treated with LPS only. (**g**) Serum TNF levels of mice that underwent sham surgery (control), subdiaphragmatic vagotomy (sVX) or splenectomy (SPX) before electroacupuncture and LPS. (**h**) Serum TNF levels in the blood from untreated mice that was supplemented *in vitro* with 50% volume of serum from donor mice that underwent sham surgery (control), electroacupuncture (EA) or adrenalectomy and electroacupuncture (ADX + EA). Top graph shows cell survival as determined by 3-(4,5-dimethylthiazol-2-yl)-2,5-diphenyltetrazolium bromide (MTT) assay. ($*P < 0.05$, Student's *t*-test, EA versus ADX + EA). (**i**) Percentage of serum TNF levels in mice treated with LPS and electroacupuncture and mice treated with LPS only in mice that underwent sham surgery (control), adrenalectomy (ADX) or treatment with reserpine. (**j**) Serum levels of catecholamines dopamine (DA), norepinephrine (NE) or epinephrine (E) from mice treated with electroacupuncture that were adrenalectomized or not. For all panels, $*P < 0.01$ ($n = 4$ per group; one-way analysis of variance (ANOVA) with Bonferroni corrections), and data are expressed as mean ± s.e.m.

suggest that the common peroneal and tibial nerves both contribute to the anti-inflammatory potential of electroacupuncture by activating the sciatic nerve. Conversely, direct electrical stimulation of the sciatic nerve mimicked the anti-inflammatory effects of electroacupuncture (**Fig. 1f**) in a voltage-dependent manner (**Supplementary Fig. 1e**), demonstrating the ability of the sciatic nerve to control systemic inflammation in sepsis.

Given that the vagus nerve inhibits cytokine production in the spleen[11,26] and prevents systemic inflammation in endotoxemia[11,26], we analyzed its contribution to the anti-inflammatory effects of electroacupuncture. Both cervical (**Supplementary Fig. 2a**) and subdiaphragmatic (**Fig. 1g**) vagotomy abolished the anti-inflammatory potential of electroacupuncture, whereas splenectomy did not prevent this effect (**Fig. 1g**). These results reveal a previously uncharacterized mechanism for vagal modulation of systemic inflammation. To define this mechanism, blood from mice given a sham operation (the same surgical procedure but without electrical stimulation) or from those that received electroacupuncture was treated *in vitro* with LPS. LPS induced TNF production in blood from sham mice but not in blood from mice treated with electroacupuncture (**Supplementary Fig. 2b**). Likewise, the serum from the mice treated with electroacupuncture attenuated *in vitro* TNF production in untreated blood (**Fig. 1h**). This anti-inflammatory potential of the serum in mice treated with electroacupuncture was prevented by adrenolectomy (**Fig. 1h**) but not by splenectomy (**Supplementary Fig. 2c**). Conversely, electroacupuncture lowered serum TNF levels in control nonadrenolectomized but not in adrenalectomized mice (**Fig. 1i**). We confirmed the role of catecholamines by using reserpine, a classical inhibitor of the vesicular monoamine transporter[26], which abolished the anti-inflammatory effects of electroacupuncture (**Fig. 1i** and **Supplementary Fig. 2d**). Electroacupuncture increased serum levels of all the three catecholamines, predominantly dopamine and norepinephrine (**Fig. 1j**). We conclude that the increase of catecholamines was mediated by the vagus nerve and the adrenal glands because either adrenalectomy (**Fig. 1j**) or cervical (**Supplementary Fig. 2e**) or subdiaphragmatic (**Fig. 2a**) vagotomy abolished the production of catecholamines. Direct electrical stimulation of the vagus nerve mimicked the production of dopamine and norepinephrine induced by electroacupuncture (**Fig. 2a**). These results establish a new mechanism for vagal modulation of inflammation mediated by the adrenal glands that is independent of the spleen. The vagal innervation of the adrenal medulla has been recently reported by retrograde tracers[27]. Although sympathetic and parasympathetic systems are considered to act in opposition to maintain physiological homeostasis, the preganglionic sympathetic neurons and vagus nerve converge in the production of acetylcholine in the adrenal medulla. Given that acetylcholine is the principal neurotransmitter of the vagus nerve and that vagal immune modulation requires the α_7 nicotinic acetylcholine receptors (α_7nAChRs)[28,29], we analyzed whether this receptor is required for electroacupuncture. α_7nAChR was not required for

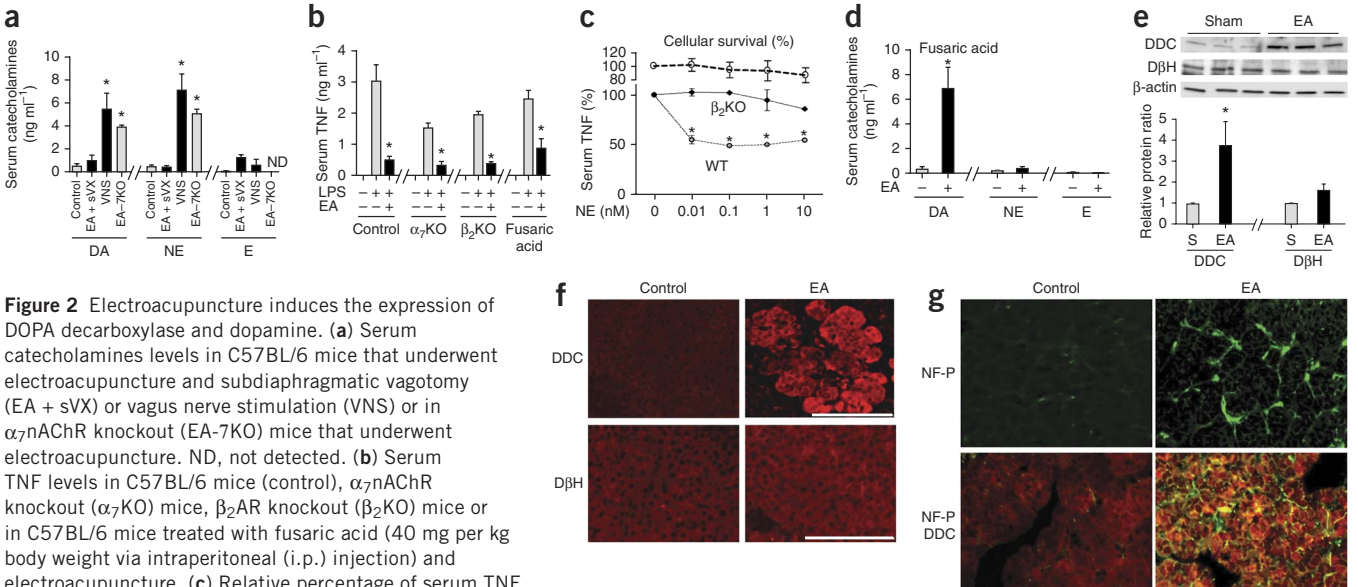

Figure 2 Electroacupuncture induces the expression of DOPA decarboxylase and dopamine. (**a**) Serum catecholamines levels in C57BL/6 mice that underwent electroacupuncture and subdiaphragmatic vagotomy (EA + sVX) or vagus nerve stimulation (VNS) or in α_7nAChR knockout (EA-7KO) mice that underwent electroacupuncture. ND, not detected. (**b**) Serum TNF levels in C57BL/6 mice (control), α_7nAChR knockout (α_7KO) mice, β_2AR knockout (β_2KO) mice or in C57BL/6 mice treated with fusaric acid (40 mg per kg body weight via intraperitoneal (i.p.) injection) and electroacupuncture. (**c**) Relative percentage of serum TNF levels in the blood from wild-type (WT) and β_2AR knockout mice treated *ex vivo* with LPS and the indicated concentrations of norepinephrine and fusaric acid (40 mg per kg body weight). (**d**) Serum levels of catecholamines dopamine, norepinephrine or epinephrine in mice treated or not with electroacupuncture. (**e**) Top, western blots for DOPA decarboxylase (DDC), dopamine β-hydroxylase (DβH) or β-actin in protein extracts from the adrenal glands of mice treated or not with electroacupuncture. Bottom, relative ratio of DDC and DβH in mice treated with electroacupuncture and mice that received sham (S). In all experiments, $*P < 0.01$ versus sham (S) ($n = 3$ per group; Student's *t*-test). (**f**) Immunostaining with anti–DOPA decarboxylase (top) and with anti–dopamine β-hydroxylase (bottom) of the adrenal medulla from mice with or without electroacupuncture. (**g**) Immunostaining with antibody to phosphorylated neurofilaments (NF-P; green, top) and costaining with antibody to phosphorylated neurofilaments (NF-P; green) and anti-DOPA decarboxylase (DDC; red, bottom) of sections of the adrenal medulla from mice treated with or without electroacupuncture. The figures are representative of three different experiments. Scale bars, 100 μm.

electroacupuncture to inhibit serum TNF levels or induce dopamine or norepinephrine (**Fig. 2a**,**b** and **Supplementary Fig. 3a**).

We analyzed the specific contribution of catecholamines using β_2 adrenoceptor (β_2AR) knockout mice. β_2 adrenoceptors are necessary receptors for the anti-inflammatory effects of norepinephrine[26]. *In vivo*, electroacupuncture inhibited serum TNF levels in both control and β_2AR knockout mice (**Fig. 2b**). However, norepinephrine inhibited TNF production in the blood from wild-type but not β_2AR knockout mice (**Fig. 2c**), indicating that norepinephrine requires β_2AR to inhibit TNF production in the blood. Together, these results indicate that electroacupuncture does not require norepinephrine to inhibit TNF production in the blood. We confirmed this hypothesis by using fusaric acid, a conventional inhibitor of the dopamine β-hydroxylase that abolishes norepinephrine production. Fusaric acid did not prevent the anti-inflammatory effects of electroacupuncture (**Fig. 2b**), but it specifically inhibited electroacupuncture-induced production of norepinephrine without affecting dopamine levels (**Fig. 2d**). By contrast, reserpine inhibited the production of both dopamine and norepinephrine and prevented the anti-inflammatory potential of electroacupuncture (**Fig. 1i**). These results suggest that dopamine has a crucial role in the anti-inflammatory potential of electroacupuncture. These results also suggest a new

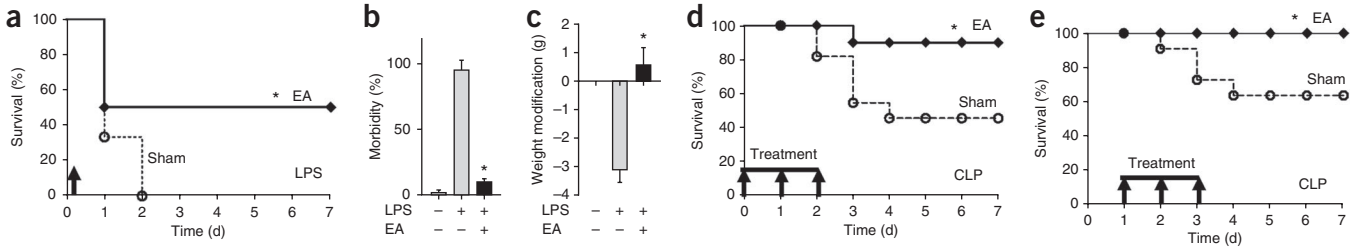

Figure 3 Electroacupuncture rescues mice from established polymicrobial peritonitis. (**a**–**c**) Adult C57BL/6 male mice underwent sham or electroacupuncture right after the LPS challenge (LPS; 12 mg per kg body weight i.p.). (**a**) Survival represented in a Kaplan-Meier analysis ($n = 20$ per group, $*P < 0.01$ survival log-rank test versus control). (**b**,**c**) Morbidity (**b**) and weight modifications (**c**) represented as mean ± s.e.m. $*P < 0.01$ ($n = 6$ per group; one-way ANOVA with Bonferroni corrections). (**d**,**e**) All mice underwent CLP and sham or electroacupuncture 15 min before (**d**) or 24 h after (**e**) the CLP. In addition to the first treatment, all mice received sham or electroacupuncture for 15 min once a day for the next 2 d. Arrows represent the treatment days. Survival is represented in a Kaplan-Meier analysis ($n = 15$ per group, $*P < 0.05$ survival log-rank test versus control). (**f**) Mice underwent surgical adrenalectomy before CLP and subsequent sham or electroacupuncture (given once a day for 3 d). Survival is represented in a Kaplan-Meier analysis ($n = 20$ per group, $*P < 0.05$ survival log-rank test versus control).

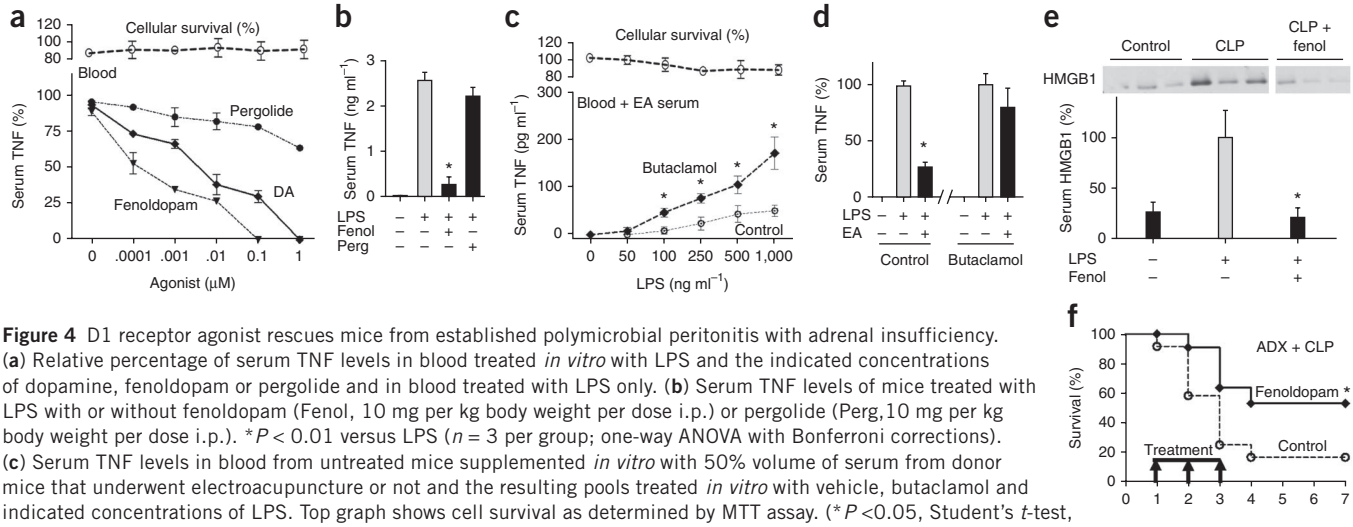

Figure 4 D1 receptor agonist rescues mice from established polymicrobial peritonitis with adrenal insufficiency. (**a**) Relative percentage of serum TNF levels in blood treated *in vitro* with LPS and the indicated concentrations of dopamine, fenoldopam or pergolide and in blood treated with LPS only. (**b**) Serum TNF levels of mice treated with LPS with or without fenoldopam (Fenol, 10 mg per kg body weight per dose i.p.) or pergolide (Perg,10 mg per kg body weight per dose i.p.). $^*P < 0.01$ versus LPS ($n = 3$ per group; one-way ANOVA with Bonferroni corrections). (**c**) Serum TNF levels in blood from untreated mice supplemented *in vitro* with 50% volume of serum from donor mice that underwent electroacupuncture or not and the resulting pools treated *in vitro* with vehicle, butaclamol and indicated concentrations of LPS. Top graph shows cell survival as determined by MTT assay. ($^*P < 0.05$, Student's *t*-test, EA versus ADX + EA). (**d**) Relative percentage of serum TNF levels in mice treated with or without LPS and electroacupuncture and given vehicle (control) or with butaclamol (12 mg per kg body weight per dose i.p.) 60 min before the LPS challenge. (**e**) Mice underwent sham (control) or CLP with vehicle (CLP) or fenoldopam (CLP + fenol). Serum HMGB1 levels were analyzed at 24 h after CLP. The graph depicts the relative percentage of serum HMGB1 levels as compared to CLP. $^*P < 0.05$ ($n = 3$ per group; mean ± s.d., one-way ANOVA with Bonferroni corrections). (**f**) Kaplan-Meier survival analysis of adrenalectomized mice with CLP treated with vehicle (control) or fenoldopam (10 mg per kg body weight per dose i.p.) started 1 d after the CLP and given every 12 h for 3 d ($n = 20$ per group, $^*P < 0.01$ survival log-rank test versus control).

role for dopamine, which is conventionally viewed in critical care as just the biological precursor of norepinephrine. In order to determine how electroacupuncture induces dopamine, we analyzed the regulation of aromatic L-amino acid (DOPA) decarboxylase (which catalyzes the formation of dopamine from L-3,4-dihydroxyphenylalanine) and dopamine β-hydroxylase (which catalyzes the degradation of dopamine to norepinephrine) in the adrenal gland. Electroacupuncture increased the levels of DOPA decarboxylase in the adrenal medulla fourfold without significantly affecting the levels of dopamine β-hydroxylase (**Fig. 2e**,**f**). It also activated the neuronal network of the adrenal medulla in the proximity of the chromaffin cells expressing high levels of DOPA decarboxylase (**Fig. 2g**).

Electroacupuncture treatment directly following the septic challenge reduced mortality, morbidity and weight loss in endotoxemic mice (**Fig. 3a**–**c**) and improved survival in mice with polymicrobial peritonitis induced by cecal ligation and puncture (CLP) (**Fig. 3d**). Furthermore, electroacupuncture also 'rescued' the mice from lethal polymicrobial peritonitis even when the treatment was started 24 h after the CLP (**Fig. 3e**). Given that recent studies reported adrenal insufficiency in patients with sepsis[4], we analyzed whether electroacupuncture improves survival in adrenolectomized mice. Adrenalectomy rendered the mice more susceptible to polymicrobial peritonitis (**Supplementary Fig. 3b**) and prevented electroacupuncture from improving survival in polymicrobial peritonitis (**Fig. 3f**).

Given that the anti-inflammatory effects of electroacupuncture are mediated by dopamine, we reasoned that dopamine agonists may mimic electroacupuncture and control inflammation in patients with sepsis and adrenal insufficiency. We analyzed the anti-inflammatory potential of dopamine using fenoldopam, a highly selective agonist for peripheral D1 receptors, and pergolide, a highly selective agonist for D2-like receptors[30,31]. Fenoldopam was more efficient than dopamine and pergolide at inhibiting LPS-induced TNF production both *ex vivo* and in mice (**Fig. 4a**,**b**). The role of D1 receptors was confirmed by using butaclamol, a standard D1 receptor antagonist[32,33], which inhibited the anti-inflammatory effects of electroacupuncture (**Fig. 4c**,**d** and **Supplementary Fig. 3c**). One dose of fenoldopam immediately following the induction of sepsis prevented mortality in polymicrobial peritonitis (**Supplementary Fig. 3d**) and lowered serum HMGB1 levels (**Fig. 4e**). As serum HMGB1 levels peak around 24 h after CLP[18], we reasoned that treatment with fenoldopam could be started after the onset of sepsis to provide a clinically relevant therapeutic time window. Treatment with fenoldopam, started 24 h after CLP, rescued mice with adrenal insufficiency from established polymicrobial peritonitis (**Fig. 4f**). We recorded survival for 3 weeks and observed no late deaths, which suggests that fenoldopam induced a lasting protection and did not merely delay the inflammatory responses. Our results concur with a randomized double-blind placebo-controlled pilot trial indicating that prophylactic fenoldopam can protect renal function in septic patients[34]. Furthermore, the present results indicate that fenoldopam can improve organ function and survival even when the treatment is started after the onset of sepsis. Together, these results suggest that dopamine D1 receptor agonists mimic the anti-inflammatory potential of electroacupuncture and can provide pharmacological advantages to control sepsis in patients with adrenal insufficiency and in a clinically relevant time frame (**Supplementary Fig. 3e**).

METHODS

Methods and any associated references are available in the online version of the paper.

Note: Any Supplementary Information and Source Data files are available in the online version of the paper.

ACKNOWLEDGMENTS

We thank P. Morcillo, J.M. Inclan-Rico and J.R. Berlin for their comments and suggestions and M. Marks (University of Colorado) and B. Kobilka (Stanford University) for the α_7nAChR and β_2AR knockout mice. R.T.-R. was supported by the University Autónoma Benito Juarez de Oaxaca. M.d.R.T.-B. was supported by the Mexican National Council for Science and Technology. L.U. is supported by the faculty program of the Department of Surgery of the New Jersey Medical School, the Foundation of University of Medicine and Dentistry of New Jersey and US National Institutes of Health grant RO1-GM084125.

AUTHOR CONTRIBUTIONS
R.T.-R., G.Y., G.P., P.M. and M.d.R.T.-B. performed the experiments, prepared the figures and revised the article. M.A.M.-E., L.A.A.-P. and A.I. contributed to the design of the study and revised the paper. L.U. designed and directed the study and wrote the paper.

COMPETING FINANCIAL INTERESTS
The authors declare no competing financial interests.

1. Angus, D.C. & van der Poll, T. Severe sepsis and septic shock. *N. Engl. J. Med.* **369**, 840–851 (2013).
2. Ulloa, L. & Tracey, K.J. The "cytokine profile": a code for sepsis. *Trends Mol. Med.* **11**, 56–63 (2005).
3. Ulloa, L. The vagus nerve and the nicotinic anti-inflammatory pathway. *Nat. Rev. Drug Discov.* **4**, 673–684 (2005).
4. Annane, D. Adrenal insufficiency in sepsis. *Curr. Pharm. Des.* **14**, 1882–1886 (2008).
5. Tracey, K.J. *et al.* Anti-cachectin/TNF monoclonal antibodies prevent septic shock during lethal bacteraemia. *Nature* **330**, 662–664 (1987).
6. Riedemann, N.C., Guo, R.F. & Ward, P.A. Novel strategies for the treatment of sepsis. *Nat. Med.* **9**, 517–524 (2003).
7. Ulloa, L., Brunner, M., Ramos, L. & Deitch, E.A. Scientific and clinical challenges in sepsis. *Curr. Pharm. Des.* **15**, 1918–1935 (2009).
8. Nathan, C. Points of control in inflammation. *Nature* **420**, 846–852 (2002).
9. Abraham, E. *et al.* Lenercept (p55 tumor necrosis factor receptor fusion protein) in severe sepsis and early septic shock: a randomized, double-blind, placebo-controlled, multicenter phase III trial with 1,342 patients. *Crit. Care Med.* **29**, 503–510 (2001).
10. Borovikova, L.V. *et al.* Vagus nerve stimulation attenuates the systemic inflammatory response to LPS. *Nature* **405**, 458–462 (2000).
11. Huston, J.M. *et al.* Splenectomy inactivates the cholinergic antiinflammatory pathway during lethal endotoxemia and polymicrobial sepsis. *J. Exp. Med.* **203**, 1623–1628 (2006).
12. Peña, G. *et al.* Cholinergic regulatory lymphocytes re-establish neuromodulation of innate immune responses in sepsis. *J. Immunol.* **187**, 718–725 (2011).
13. Bernik, T.R. *et al.* Cholinergic antiinflammatory pathway inhibition of tumor necrosis factor during ischemia reperfusion. *J. Vasc. Surg.* **36**, 1231–1236 (2002).
14. Altavilla, D. *et al.* Activation of the cholinergic anti-inflammatory pathway reduces NF-kappab activation, blunts TNF-α production, and protects againts splanchic artery occlusion shock. *Shock* **25**, 500–506 (2006).
15. Cai, B. *et al.* α_7 cholinergic-agonist prevents systemic inflammation and improves survival during resuscitation. *J. Cell. Mol. Med.* **13**, 3774–3785 (2009).
16. van Westerloo, D.J. *et al.* The vagus nerve and nicotinic receptors modulate experimental pancreatitis severity in mice. *Gastroenterology* **130**, 1822–1830 (2006).
17. Pullan, R.D. *et al.* Transdermal nicotine for active ulcerative colitis. *N. Engl. J. Med.* **330**, 811–815 (1994).
18. Wang, H. *et al.* Cholinergic agonists inhibit HMGB1 release and improve survival in experimental sepsis. *Nat. Med.* **10**, 1216–1221 (2004).
19. van Westerloo, D.J. *et al.* The cholinergic anti-inflammatory pathway regulates the host response during septic peritonitis. *J. Infect. Dis.* **191**, 2138–2148 (2005).
20. Vickers, A.J. *et al.* Acupuncture for chronic pain: individual patient data meta-analysis. *Arch. Intern. Med.* **172**, 1444–1453 (2012).
21. Lee, A. & Done, M.L. Stimulation of the wrist acupuncture point P6 for preventing postoperative nausea and vomiting. *Cochrane Database Syst. Rev.* CD003281 (2004).
22. Napadow, V. & Kaptchuk, T.J. Patient characteristics for outpatient acupuncture in Beijing, China. *J. Altern. Complement. Med.* **10**, 565–572 (2004).
23. Wu, H.M. *et al.* Acupuncture for stroke rehabilitation. *Cochrane Database Syst. Rev.* CD004131 (2006).
24. Goldman, N. *et al.* Adenosine A1 receptors mediate local anti-nociceptive effects of acupuncture. *Nat. Neurosci.* **13**, 883–888 (2010).
25. Ernst, E., Lee, M.S. & Choi, T.Y. Acupuncture: does it alleviate pain and are there serious risks? A review of reviews. *Pain* **152**, 755–764 (2011).
26. Vida, G. *et al.* β_2-Adrenoreceptors of regulatory lymphocytes are essential for vagal neuromodulation of the innate immune system. *FASEB J.* **25**, 4476–4485 (2011).
27. Coupland, R.E., Parker, T.L., Kesse, W.K. & Mohamed, A.A. The innervation of the adrenal gland. III. Vagal innervation. *J. Anat.* **163**, 173–181 (1989).
28. Wang, H. *et al.* Nicotinic acetylcholine receptor α_7 subunit is an essential regulator of inflammation. *Nature* **421**, 384–388 (2003).
29. Vida, G., Peña, G., Deitch, E.A. & Ulloa, L. α_7-nicotinic receptor mediates vagal induction of splenic norepinephrine. *J. Immunol.* **186**, 4340–4346 (2011).
30. Grenader, A. & Healy, D.P. Fenoldopam is a partial agonist at dopamine-1 (DA1) receptors in LLC-PK1 cells. *J. Pharmacol. Exp. Ther.* **258**, 193–198 (1991).
31. Weber, R.R. *et al.* Pharmacokinetic and pharmacodynamic properties of intravenous fenoldopam, a dopamine1-receptor agonist, in hypertensive patients. *Br. J. Clin. Pharmacol.* **25**, 17–21 (1988).
32. Denef, C., Manet, D. & Dewals, R. Dopaminergic stimulation of prolactin release. *Nature* **285**, 243–246 (1980).
33. Gorissen, H. & Laduron, P. Solubilisation of high-affinity dopamine receptors. *Nature* **279**, 72–74 (1979).
34. Morelli, A. *et al.* Prophylactic fenoldopam for renal protection in sepsis: a randomized, double-blind, placebo-controlled pilot trial. *Crit. Care Med.* **33**, 2451–2456 (2005).

ONLINE METHODS

Chemicals and reagents. LPS (*Escherichia coli* 0111:B4), capsaicin, reserpine, fusaric acid, dopamine, fenoldopam, pergolide and butaclamol were all purchased from Sigma-Aldrich (Saint Louis, MO) and dissolved in sterile pyrogen-free PBS (Gibco, Life Technologies, Grand Island, NY). Capsaicin (5 mg per kg body weight via intramuscular (i.m.) injection; dissolved in PBS with 10% ethyl alcohol) was administered at 72 h and 48 h before the LPS challenge. Reserpine (5 mg per kg body weight i.p.; dissolved in 25% DMSO-PBS) was injected at 24 h before the lethal endotoxemia. Fusaric acid (40 mg per kg body weight per dose i.p.) was administered at 8 h and 4 h before the LPS challenge. Fenoldopam (10 mg per kg body weight per dose i.p.) was injected at 30 min and 5 min before LPS administration. Pergolide (10 mg per kg body weight per dose i.p.; dissolved in 25% DMSO-PBS) was given at 12 h and 5 min before the LPS challenge. Butaclamol (12 mg per kg body weight i.p) was given 60 min before the endotoxemic challenge. *In vitro*, dopamine, fenoldopam, pergolide and butaclamol were used at 5 min before the LPS challenge at the concentration indicated in the figures.

Animal experiments. Animal procedures were approved by the Institutional Animal Care & Use Committee of the New Jersey Medical School of Rutgers University. All animal experiments were performed in 6- to 8-week-old (~25 ± 5 g) male mice without any exclusion criteria. Wild-type C57BL/6 male mice were obtained from The Jackson Laboratory (Bar Harbor, ME). α_7nAChR knockout (Chrna7^{tm1Bay}) mice and wild-type littermates[29] were obtained from M. Marks. β_2AR knockout (Adrb2^{tm1Bkk}) mice and wild-type littermates were obtained from B. Kobilka[26]. α_7nAChR and β_2AR knockout mice were bred and genotyped by PCR using genomic DNA from mouse tails and the Extract-N-Amp Tissue PCR kit (Sigma Chemical, Saint Louis, MO) as we previously described[32,35]. Mice were randomly distributed to ensure same age and sample size in different groups for experimental treatment. The investigators were blinded to the experimental treatments. Mice were maintained on 12-h light-dark cycle, with free access to food and water (*ad libitum*).

Experimental sepsis. Endotoxemia and CLP were performed as we previously described[18]. LPS (*E. coli* LPS 0111:B4; Sigma Chemical, Saint Louis, MO) was dissolved in sterile pyrogen-free PBS (Gibco: Life Technologies, Grand Island, NY) and sonicated for 30 min immediately before use. Mice received a LD_{50} dose (dose lethal to 50% of mice tested) of LPS (6 mg per kg body weight i.p.). LPS was added to the whole blood to a final concentration of 250 ng ml^{-1} for the *in vitro* procedures. CLP is the most clinically relevant experimental model of sepsis because the inflammatory responses are induced by both polymicrobial peritonitis caused by the cecal puncture and the necrotic tissue produced by the cecal ligation. Mice were anesthetized with ketamine (60 mg per kg body weight i.p.; Fort Dodge, Fort Dodge, IA) and xylazine (5 mg per kg body weight i.p.; Boehringer Ingelheim, St. Joseph, MO) and subjected to a standard CLP procedure with 50% average mortality rate as we previously described[18]. An abdominal incision of approximately 1.0 cm was performed to expose and ligate the cecum at 5.0 mm from the cecal tip away from the ileocecal valve. The ligated cecal stump was punctured only once with a 22-gauge needle, and the stool was extruded (~1.0 mm) to ascertain patency of puncture. The abdominal wound was closed in two layers, peritoneum and fascia (separately), to prevent leakage of fluid. All mice received antibiotic (enrofloxacine 0.9 mg per kg body weight subcutaneously; Baytril, Bayer Health Care, Swanee Mission, KA) dissolved in 0.9% normal saline immediately after surgery and every 12 h for 3 d.

Selective neurectomies and electrical stimulations. All selective neurectomies and electrical stimulations were performed in mice anesthetized with ketamine (60 mg per kg body weight i.p.; Fort Dodge, Fort Dodge, IA) and xylazine (5 mg per kg body weight i.p.; Boehringer Ingelheim, St. Joseph, MO). The electrical stimulation in electroacupuncture and direct nerve stimulation (sciatic and vagus nerves) was performed with a continuous-mode stimulation for 15 min with a electrical potential difference of 4 V, an electric current of 40 mA, a pulse width of 50 μs and a frequency of 10 Hz using the electrostimulator (STM 150, Biopac Systems, Goleta, CA) controlled with the AcqKnowledge Lab Assistant GLP software (ACK100W-G, Biopac Systems, Goleta, CA). The data were processed with the MP150 Data Acquisition System (MP150WSW, Biopac Systems, Goleta, CA). Control mice underwent a sham surgery with the same surgical procedure but without the electrical stimulation. Electroacupuncture was performed similar to that described by Goldman *et al.*[24]. Electroacupuncture was performed by stimulating both limbs at the ST36 Zusanli acupoint by inserting each 12-mm unipolar stainless steel needle electrode (EL452, Biopac Systems, Goleta, CA) about 3 mm deep in each acupoint. The ST36 Zusanli acupoint is located 2 mm lateral to the anterior tubercle of the tibia in the anterior tibial muscle and 4 mm distal to the knee joint lower point. The ST36 Zusanli acupoint is located in the proximity of the common peroneal and tibial branches of the sciatic nerve[34,35]. Control treatments included the same procedure but using a non-electrical wooden 'toothpick' instead of the electrodes. Additional control treatments were performed by stimulating a distal nonacupoint. This nonacupoint is ~3 cm distal from the ST36 acupoint toward the tail and opposite to the knee joint. It is located over the semitendinosus muscle at 5 mm from the tail base. This nonacupoint is neither referred in the acupoint map of rodents nor close to any major nerve. For peroneal or tibial neurectomy, the dissection of the peroneal or tibial nerve was done as previously described[36]. A thigh incision was performed on its external face to expose the artery parallel to the femur. The quadriceps muscles were dissected to expose the common peroneal and the tibial branches of the sciatic nerve. The selective neurectomy of the common peroneal or the tibial branches was performed by exposing the nerve and stabilizing it with nylon thread, followed by surgical sectioning of the nerve. The nerves were dissected 72 h before the electroacupuncture. In control sham-operated mice, the respective nerves were exposed and isolated from the surrounding tissue, but not transected. For sciatic neurectomy before electroacupuncture, a dorsal incision of ~1 cm was performed next to the posterior median line between the second and the fifth lumbar vertebrae. The latissimus dorsi muscle between the third and fifth lumbar vertebrae was dissected to expose the sciatic nerve branches on both sides of the dorsal root. The sciatic nerve branches were stabilized with nylon thread and cut just distal to the dorsal root ganglions. The sciatic nerve was sectioned 72 h before the electroacupuncture. For sciatic nerve stimulation, the sciatic nerve was exposed as described above, the nerve was not transected and the bipolar electrode was placed at the greater ischeal notch of the sciatic nerve for the electrical activation. Cervical vagotomy was performed as we previously described[29]. Mice were subjected to an anterior incision on the neck to access the sternocleidomastoid muscle. The sternocleidomastoid muscle was dissected to visualize the carotid artery and the vagus nerve. The vagus nerve branches on both sides of the neck were stabilized with nylon thread and cut. Subdiaphragmatic vagotomy was performed as we previously described[11]. Mice underwent an abdominal incision covering the epigastrium and mesogastrium. The esophagus was exposed at the juncture to the stomach. Subsequently, the two vagal branches on both sides of the dorsal part of the esophagus were exposed by gently pulling down and twisting the stomach and stabilizing with nylon thread. Both vagal branches were then cut 72 h before the experimental procedure. Vagus nerve stimulation was performed similar to what we have previously described[11]. The subdiaphragmatic vagal branches were exposed as described above, and the two vagal branches on both sides of the dorsal part of the esophagus were exposed by gently pulling down and twisting the stomach. Both vagal branches were stabilized with nylon thread and transected 72 h before the stimulation, and the bipolar electrode was placed across the base of the esophagus to the distal tips of the vagal nerves.

Ablative surgeries. All mice were anesthetized with ketamine (60 mg per kg body weight i.p.; Fort Dodge, Fort Dodge, IA) and xylazine (5 mg per kg body weight i.p.; Boehringer Ingelheim, St. Joseph, MO) before the surgical procedures. Splenectomy was performed as we have previously described[11]. Anesthetized mice were subjected to an abdominal incision on the epigastrium and mesogastrium. The spleen was exposed by gentle retraction of the stomach to the side. The three main branches of the spleen artery were stabilized with nylon thread, ligated and cut. The spleen was removed and the wound was closed with sutures: catgut for the abdominal wall and nylon thread for the skin. Mice were splenectomized 3 d before the experimental procedure. Adrenalectomy was performed as described[29]. A dorsal incision from the

doi:10.1038/nm.3479

first to the third lumbar vertebrae was performed on anesthetized mice. The latissimus dorsi muscle was dissected and pulled away on both sides until the kidneys were visible. Both adrenal glands and their adipose tissue were removed. Adrenalectomized mice were given drinking water with 0.9% NaCl for 10 d before the experimental procedure.

Morbidity. The score is based on the specific endpoints previously described[37]. Characteristic clinical manifestations of endotoxemia (piloerection, exudates around the eyes and nostrils, lethargy, diarrhea and diminished locomotor activity) were scored by three independent researchers blinded to the treatment. A four-point score was used for lethargy and diminished locomotor activity (low, low-moderate, moderate and severe) and a two-point score (absent or present) for the evaluation of hypothermia, exudates around the eyes and/or nostrils, diarrhea and piloerection.

Cytokine analyses. For *in vivo* serum analyses, blood was collected at the indicated time points, allowed to clot for 2 h at room temperature and centrifuged at 2,000*g* for 15 min at 4 °C. *In vivo*, serum TNF concentrations were analyzed in the serum of the endotoxemic mice at 90 min (or the specific time points indicated in **Fig. 1**) after LPS challenge using the TNF ELISA Kit (eBioscience, San Diego, CA). IL-6, MCP-1 and INF-γ were analyzed at the indicated time points with Cytometric Bead Array Mouse Inflammation Kit (BD Bioscences, San Jose, CA). Blood catecholamines were determined by ELISA (Rocky Mountain Diagnostics, Colorado Springs, CO) at 15 min after stimulation as we previously described[26,29]. For the *in vitro* experiments, blood was collected by cardiac puncture in heparin microtainer, placed in 96-well cell culture plates (Greiner bio-one, CELLSTAR, BioExpress, Kaysville, UT) and incubated with equal volume of RPMI medium (Gibco, Life Technologies, Grand Island, NY) or experimental serum for 15 min before the LPS challenge. Next, the samples were centrifuged (800*g* for 5 min at room temperature), and the cytokines were analyzed in the conditioned supernatant. *In vitro*, TNF was analyzed in the conditioned supernatant at 3 h after the LPS challenge. Cytokine analyses in the conditioned medium were performed using the same reagents as reported above.

Cytotoxicity. Cell cytoxicity was analyzed using MTT (3-(4,5-dimethylthiazol-2-yl)-2,5-diphenyltetrazolium bromide, a yellow tetrazole) colorimetric assay. Cells were incubated for 2 h with 10% of the 5 mg/ml MTT solution dissolved in PBS. Next, cells were treated with 200 µl of solubilizer solution (isopropanol, HCl and Triton X-100) to dissolve the formazan crystals. The absorbance at 540 nm was determined.

Immunofluorescence. Immunofluorescence imaging was performed as previously described[38]. The adrenal glands from mice treated with fusaric acid were collected, fixed overnight in 4% paraformaldehyde solution in PBS (USB, Affimetrix, Santa Clara, CA) and embedded in paraffin wax. Sections were cut at a thickness of 5 µm with a microtome (Leica RM2235, Leica Microsystems Inc., Buffalo Grove, IL). Sections were dewaxed in xylene and rehydrated by a series of ethanol-water washes. Antigen retrieval was performed by incubating the sections in retrieval buffer (10 mM Tris base, 1 mM EDTA solution, 0.05% Tween 20, pH 9.0) at 100 °C for 20 min. Sections were blocked in a solution of 10% FBS with 1% BSA (Sigma Chemical, Saint Louis, MO) for 2 h at room temperature. Next, the sections were incubated with primary antibodies to DOPA decarboxylase (1:1,000, ab3905, Abcam, Cambridge, MA) or dopamine β-hydroxylase (1:1,000, ab43868 Abcam, Cambridge, MA) or SMI310 primary antibody to phosphorylated neurofilaments (1:1,000, ab24570 Abcam, Cambridge, MA) diluted in 1% BSA-TBST (0.1% Tween 20, Tris-buffered saline, pH 7.4) for 1 h at room temperature. Subsequently, the sections were washed four times in TBST for 5 min each wash and incubated with FITC-conjugated goat antibody to mouse IgG (1:250, AP124F, Millipore, Temecula, CA) or AlexaFluor 568–conjugated goat antibody to rabbit IgG (H+L) (1:500, A-11011, Molecular Probes, Life Technologies, Grand Island, NY) diluted in 1% BSA-TBST for 1 h at room temperature in the dark. The slides were washed four times in TBST for 5 min each wash and mounted with Vectashield Mounting Media (Vector Laboratories, Burlingame, CA). Next, the slides were analyzed with the Nikon A1R-A1 Confocal Microscope System (Nikon Instruments, Melville, NY) providing a wavelength of 488 nm and 561 nm to excite the FITC– and AlexaFluor 568–labeled antibodies, respectively.

Western blot. Western blot assay was performed similarly as we described[39] The adrenal glands were homogenized (1:20 w/v) in lysis buffer with protease inhibitor (CelLyticMT and Protease Inhibitor Cocktail P8340; 1:100 v/v, both from Sigma-Aldrich, Saint Louis, MO) and centrifuged at 16,000*g* for 15 min at 4 °C. Protein concentration in the supernatant was analyzed using the Bio-Rad Protein Assay (Bio-Rad, Life Science Research, Hercules, CA). 30 µg of protein sample was loaded per lane for SDS-PAGE analyses. Samples were run on the NuPAGE Bis-Tris Mini Gels (Novex, Invitrogen, Life Technologies, Grand Island, NY) at 200 V for 50 min. The samples were transferred onto the PVDF membranes (Hybond-P, Amersham, GE Healthcare, Pittsburg, PA) by using the iBlot Gel Transfer Device (Invitrogen, Life Technologies, Grand Island, NY). The membranes were blocked with 5% BSA-TBST for 1 h at 4 °C and incubated with antibody to DOPA decarboxylase (1:1,000, ab3905, Abcam, Cambridge, MA), antibody to dopamine β-hydroxylase (1:1,000, ab43868, Abcam, Cambridge, MA) or anti–β-actin (1:1,000, 13E5, Cell Signaling, Danvers, MA) overnight at 4 °C. The membranes were washed five times for 5 min with TBST and incubated with HRP-linked antibody to rabbit IgG (1:1,000, #7074, Cell Signaling, Danvers, MA) at room temperature for 1 h. The membranes were washed again five times for 5 min in TBST and processed using the SuperSignal West Femto Chemiluminescent Substrate kit (Thermo Fisher Scientific, Waltham, MA). The X-ray films were scanned, and the signal density was quantified using ImageJ software (NIH Image program, Bethesda, MD).

Statistical analyses. All tests were performed using the GraphPad Prism Software (GraphPad Software, La Jolla, CA). Sample size was determined using s.d. values and power analyses of our previous studies on the vagus nerve stimulation[11,29]. All data in the figures and text are expressed as mean ± s.e.m except where depicted. Statistical analyses were performed using the one-way ANOVA with multiple pairwise comparisons with the Bonferroni adjustment for multiple hypothesis testing. Normality and homogeneity of variance were confirmed using the Kolmogorov-Smirnov analysis. ANOVA was used to compare all treatments and specific pairwise comparisons as stated in the experiments. Student's *t*-test (Mann-Whitney *U*-test) was used to compare mean values between two experimental groups. Statistical analyses of survival were determined using the log-rank test. P values <0.05 were considered statistically significant.

35. Sorkin, L.S. & Yaksh, T.L. Behavioral models of pain states evoked by physical injury to the peripheral nerve. *Neurotherapeutics* **6**, 609–619 (2009).
36. Richner, M., Bjerrum, O.J., Nykjaer, A. & Vaegter, C.B. The spared nerve injury (SNI) model of induced mechanical allodynia in mice. *J. Vis. Exp.* 3092 (2011).
37. Kadl, A., Pontiller, J., Exner, M. & Leitinger, N. Single bolus injection of bilirubin improves the clinical outcome in a mouse model of endotoxemia. *Shock* **28**, 582–588 (2007).
38. Panayotis, N. *et al.* Morphological and functional alterations in the substantia nigra pars compacta of the Mecp2-null mouse. *Neurobiol. Dis.* **41**, 385–397 (2011).
39. Ulloa, L., Doody, J. & Massague, J. Inhibition of transforming growth factor-beta/SMAD signalling by the interferon-gamma/STAT pathway. *Nature* **397**, 710–713 (1999).